

## 1 **CSPAD-140k - a Versatile Detector for LCLS Experiments**

2 Sven Herrmann<sup>a</sup>, Sébastien Boutet<sup>b</sup>, Brian Duda<sup>a</sup>, David Fritz<sup>b</sup>, Gunther Haller<sup>a</sup>, Philip Hart<sup>a</sup>, Ryan Herbst<sup>a</sup>  
3 Christopher Kenney<sup>a</sup>, Henrik Lemke<sup>b</sup>, Marc Messerschmidt<sup>b</sup>, Jack Pines<sup>a</sup>, Aymeric Robert<sup>b</sup>, Marcin  
4 Sikorski<sup>b</sup>, Garth Williams<sup>b</sup>

5 <sup>a</sup> SLAC National Accelerator Laboratory, Menlo Park, CA 94025, USA

6 <sup>b</sup> LCLS, SLAC National Accelerator Laboratory, Menlo Park, CA 94025, USA

7 corresponding author: Sven Herrmann, [herrmann@slac.stanford.edu](mailto:herrmann@slac.stanford.edu), tel: +1 650 926-2983

8 SLAC National Accelerator Laboratory, 2575 Sand Hill Road, MS-94, Menlo Park, CA 94025, USA

9 potential referees:

10 Rainer Richter, [rar@hll.mpg.de](mailto:rar@hll.mpg.de) (MPI for physics, Munich, Germany)

11 Bernd Schmitt, [bernd.schmitt@psi.ch](mailto:bernd.schmitt@psi.ch), (Paul Scherrer Institut, Villigen, Switzerland)

12 Peter Siddons, [siddons@bnl.gov](mailto:siddons@bnl.gov), (Brookhaven National Lab, USA)

13

### 14 **Abstract**

15 With the successful operation of three 2.3 megapixel, 120Hz readout rate, hybrid pixel array detectors  
16 at the Linac Coherent Light Source (LCLS), the SLAC National Accelerator Laboratory detector group is  
17 now exploring additional applications based on the same detector platform. These megapixel cameras  
18 are based on the Cornell-SLAC hybrid Pixel Array Detector (CSPAD).

19 The CSPAD platform is developed around the CSPAD ASIC, a 36 kilopixel device, each pixel at  
20  $110 \times 110 \mu\text{m}^2$ . Important characteristics of the CSPAD (room temperature operation, 14bit on chip  
21 digitization with a purely digital data interface, and scaling modularity) make it an effective choice for  
22 designing detector variants that are optimized for a range of experiments and applications.

23 One of the first spin-off detectors based on this proven CSPAD platform is the CSPAD-140k: a 140  
24 kilopixel detector, with an active area of approximately  $4 \times 4 \text{cm}^2$  and four ASICs, bundled in a small,  
25 inexpensive and easy-to-deploy package. Due to its versatility it has already been used successfully in  
26 several experiments at the CXI, XPP and XCS instruments at LCLS. The work also describes problems  
27 faced by scaling from a prototype system to a full size x-ray camera and presents the current status on  
28 the improvements achieved.

29

30 Keywords: hybrid pixel detector; free electron laser; electronics; ASIC; CSPAD;

### 31 **Introduction**

32 With the successful operation of three 2.3 megapixel, 120Hz readout rate, hybrid pixel array detectors  
33 at the Linac Coherent Light Source (LCLS), the SLAC National Accelerator Laboratory detector group is  
34 now exploring additional applications based on the same detector platform. These megapixel cameras  
35 are based on the Cornell-SLAC hybrid Pixel Array Detector (CSPAD) [1][2][3], particularly the hybrid pixel  
36 detector ASIC. This ASIC, with  $194 \times 185$  pixels of  $110 \times 110 \mu\text{m}^2$  size, is the central component of the  
37 CSPAD platform. Two ASICs, bump bonded to a single  $500 \mu\text{m}$ -thick high-resistivity silicon pixel array  
38 sensor, constitute a  $2 \times 1$  module, which is the basic building block of all CSPAD cameras. The first  
39 detector variant based on this proven platform, the CSPAD-140k, uses two of these blocks, glued to a  
40 carrier, building up a  $2 \times 2$  module with a total of about 140 kilopixels. The CSPAD-140k (Figure 1) is a 140  
41 kilopixel detector, with an active area of approximately  $4 \times 4 \text{cm}^2$ , bundled in a small, low-cost and easy-

42 to-deploy package, suitable for various synchrotron and FEL applications. Development and  
43 performance optimization of this detector will be discussed in the following paragraphs.

44 (Figure 1 here; caption: The CSPAD 140k detector, an evolution of the pixel array detectors used  
45 successfully with megapixel cameras at LCLS.)

46

## 47 **Electronics and ASIC**

48 The pixel architecture is shown in Figure 2. It consists of a charge sensitive amplifier with two gain  
49 settings for collecting the detected signal. The sample and hold stage captures the amplifier output  
50 voltage and stores it for digitization. A comparator triggers when an externally supplied ramp falls below  
51 the stored signal voltage. A counter counts the clock cycles from the ramp start to the time point when  
52 the comparator fires. This implements a single slope analog to digital (A/D) converter. The counter  
53 values of all pixels are then readout one after the other.

54 (Figure 2 here; caption: Circuit diagram for a single CSPAD pixel. Functional elements in this circuit are  
55 described in the text.)

56 Basic parameters of the CSPAD ASIC are summarized in Table 1 and [1][2][3].

57	pixel size	110 $\mu$ m x 110 $\mu$ m
58	ASIC size	185 x 194 pixels
59	frame rate	120Hz
60	effective noise	300e- in HG; 1000e- in LG
61	single 8keV Photon SNR	7 in HG; 2 in LG
62	maximum photon count	350 in HG; 2700 in LG

63 [Table 1; caption: Basic physical and performance parameters of the CSPAD ASIC. (HG: high gain, LG: low  
64 gain mode)]

65 The first measurements performed at LCLS with a large 2.3 megapixel camera revealed that the single  
66 photon gain is smaller than expected from simulations and measurements with the prototype system. A  
67 comparison is shown in Figure 3. (Figure 3 here; caption: Comparison of a Monte Carlo simulated pixel  
68 histogram and a measured histogram. The Monte Carlo simulation used the CSPADs design parameters.  
69 The measurement was performed with an early 2.3 megapixel CSPAD version. The histogram shows the  
70 noise peak and the single 8keV photon peak. The measured gain for small signals is 4 times smaller than  
71 expected.) Further studies with these cameras showed complex crosstalk behavior between the pixels,  
72 partially due to on-chip and partially due to chip-PC-board-system interaction. The CSPAD-140k is  
73 especially suited for debugging these effects, as the 2x2 module with 4 ASICs is considerably simpler  
74 than the 2.3 megapixel cameras with 64 ASICs, while still using similar electronics and power cycling  
75 features. The electronics used in the CSPAD-140k are also much more easily accessible for probing or  
76 making modifications.

77 Figure 4 shows the measured ramp function with and without the ASIC. It can be seen that the firing of  
78 all the comparators within a short time modifies the external ramp signal. The modified ramp shows an  
79 undershoot, which accelerates the firing of comparators that have not yet reached their firing level.  
80 (Figure 4 here; caption: Screenshot of the ramp measured with and without the ASICs. The difference  
81 between the two ramp functions is shown in the lower trace with a fivefold magnification of the  
82 amplitude. The ramp exhibits undershoot when most of the comparators fire and the counters stop

83 counting.) Another aspect of this inter-pixel crosstalk is the modification of the ASIC bias voltages. Figure  
84 5 shows the four external bias nodes during the A/D conversion process. (Figure 5 here; caption:  
85 Screenshot of the ASIC bias nodes during the A/D conversion process. When most pixels stop counting  
86 the comparator bias nodes exhibit undershoot.) When most of the comparators fire, the bias voltage  
87 nodes of the comparators exhibit undershoot. This undershoot increases the effective bias current in  
88 the comparators, which in turn makes the comparators faster and therefore fire earlier, increasing the  
89 correlation of comparator firing. This effect is amplified by the on-board circuitry that is needed for  
90 power cycling the LCLS 2.3 megapixel CSPAD cameras: in order to switch the biases on and off at a rate  
91 of 120Hz, the nodes cannot simply be tied to a constant voltage. The local power regulators, which have  
92 to serve up to 16 ASICs, cannot respond fast enough to sudden changes in supply current when many  
93 counters stop clocking. In the current compact camera design, the impulse response on the power  
94 nodes feeds through to the ramp generation circuitry.

95 The small signal gain of a pixel depends on the actual ramp steepness the pixel sees around its pedestal  
96 value, and therefore on the comparator firing time. Figure 6 shows the measured variation of the gain  
97 of a pixel plotted against its average pedestal value (Figure 6 here; caption: Measured variation of the  
98 gain of a CSPAD pixel plotted against its average pedestal value. After the first pixel comparators fire the  
99 gain breaks down and most pixels show a small gain. Pixels with comparators which fire late show  
100 almost nominal gain). It can be seen that the majority of the pixels exhibit a smaller gain for small  
101 signals. This apparent smaller gain also affects the measured noise. In contrast, large signals will show  
102 the real gain. Furthermore, a camera showing the above effects can exhibit large signal crosstalk when  
103 areas of an ASIC are heavily illuminated, resulting in pedestal changes of the non-illuminated regions. As  
104 designed, the comparators in illuminated pixels fire later; therefore, their crosstalk contribution is  
105 missing at the time the comparators of the non-illuminated pixels fire. Due to this sequence, the  
106 comparators in the non-illuminated regions will fire on average a bit later, resulting in an unexpected  
107 increase of their digital pedestal value.

108 Modifications in the PCB power supply and improved bias and ramp generation have helped mitigate  
109 pixel crosstalk, and the new resulting cameras show a behavior much closer to the expected  
110 performance. As an example of the improved performance, Figure 7 shows a single photon histogram of  
111 copper fluorescence from a typical pixel measured with the CSPAD-140k. (Figure 7 here; caption:  
112 Measured histogram of a CSPAD-140k pixel illuminated with copper fluorescence in high gain mode.)

### 113 **CSPAD-140k: camera and applications at LCLS**

114 The pulsed nature of the LCLS allows using very short integration times. The CSPAD's hybrid pixel design  
115 enables electronic shuttering with signal integration times in the microsecond range; therefore, the  
116 detector can operate at room temperature without performance degradation from leakage current. For  
117 operation in vacuum, the temperature is stabilized by water cooling. For applications which need longer  
118 integration times, like experiments at synchrotrons, the design also supports utilization of a Peltier  
119 element to cool the detector. Figure 1 shows the basic elements of the CSPAD-140k camera. The camera  
120 housing, which includes the detector-ASIC hybrid and support electronics, is approximately 23.6cm long,  
121 4.4cm wide and 4.8cm tall. Behind a black kapton window is a 2x2 module with approximately 4cm x  
122 4cm active area and about 140 kilopixels. The CSPAD-140k module uses a fiber-optic interface to  
123 transfer data to the data acquisition system. Power and trigger signals are routed via a 26pin DSUB  
124 connector. The result is a small but robust interface which enables convenient deployment of the  
125 detector in an experiment chamber.

126 A variant designed with slight modification to the package has been built for installation at the MEC  
127 instrument, where it will be used as a suitable alternate detector capable of 120Hz readout, replacing a  
128 slow CCD camera in a Thomson spectrometer setup. Figure 8 shows a drawing of the MEC spectrometer  
129 with the CSPAD-140k (Figure 8; caption: View of a CSPAD-140k integrated as detector of a spectrometer  
130 in which will be used by the MEC instrument at LCLS).

131 A major advantage of the small and modular design of the CSPAD-140k is the capability to deploy  
132 multiple detectors in various mechanical arrangements. An interesting application of multiple CSPAD-  
133 140k modules is to tile them into an arc-like configuration in order to cover a larger angle relative to the  
134 interaction point. The multiple single-detector units represent a dedicated compound detector from the  
135 data acquisition system point of view. Figure 9 shows the concept for an upcoming experiment at the  
136 CXI instrument at LCLS (Figure 9; caption: View of an array of CSPAD-140k detectors organized in a  
137 compound detector; this design is under consideration for an upcoming experiment using the CXI  
138 instrument at LCLS).

139 The CSPAD-140k has already been used successfully in several experiments using the CXI [4], XPP and  
140 XCS instruments at LCLS. As an example, Figure 10 shows a single shot small angle scattering image  
141 recorded with CSPAD-140k using the XCS instrument. A dried colloidal dispersion was illuminated with  
142 unfocused monochromatic beam of 9.48keV energy. The detector was located 7.8m behind the sample.

143 (Figure 10; caption: Single shot image recorded with the CSPAD-140k using the XCS instrument of LCLS.  
144 A dried colloidal dispersion is illuminated with the LCLS unfocused beam at 9.48keV energy. The  
145 detector was located 7.8m behind the sample).

## 146 **Conclusions**

147 A small versatile x-ray camera based on the CSPAD platform has been built at SLAC. This system helped  
148 to characterize and improve the performance of all CSPAD cameras. In addition the CSPAD-140k has  
149 already been used for several experiments at LCLS and many more applications for this detector at  
150 synchrotrons and FELs are expected.

151

## 152 **Acknowledgements**

153 This work is supported by the Department of Energy, Laboratory Directed Research and Development  
154 funding, under contract DE-AC02-76SF00515. Portions of this research were carried out at the Linac  
155 Coherent Light Source, a National User Facility operated by Stanford University on behalf of the U.S.  
156 Department of Energy (DOE), Office of Basic Energy Sciences (OBES)

157

## 158 **References**

159 [1] L.J. Koerner, H.T. Philipp, M.S. Hromalik, M.W. Tate, S.M. Gruner, X-ray tests of a Pixel Array Detector  
160 for coherent x-ray imaging at the Linac Coherent Light Source, J Instrum, 4 (2009).

161 [2] H.T. Philipp, M. Hromalik, M. Tate, L. Koerner, S.M. Gruner, Pixel array detector for X-ray free  
162 electron laser experiments, Nucl Instrum Meth A, 649 (2011) 67-69.

163 [3] L.J. Koerner, M.S. Hromalik, M.W. Tate, S.M. Gruner, Femtosecond Radiation Experiment Detector  
164 for X-Ray Free-Electron Laser (XFEL) Coherent X-Ray Imaging, IEEE Transactions on Nuclear Science, 57  
165 (2010) 5p.

166 [4] R. Alonso-Mori et al, Shot-by-Shot Energy-Dispersive X-ray Emission Spectroscopy Using an X-ray Free  
167 Electron Laser. Submitted for publication.

Figure 1  
[Click here to download high resolution image](#)

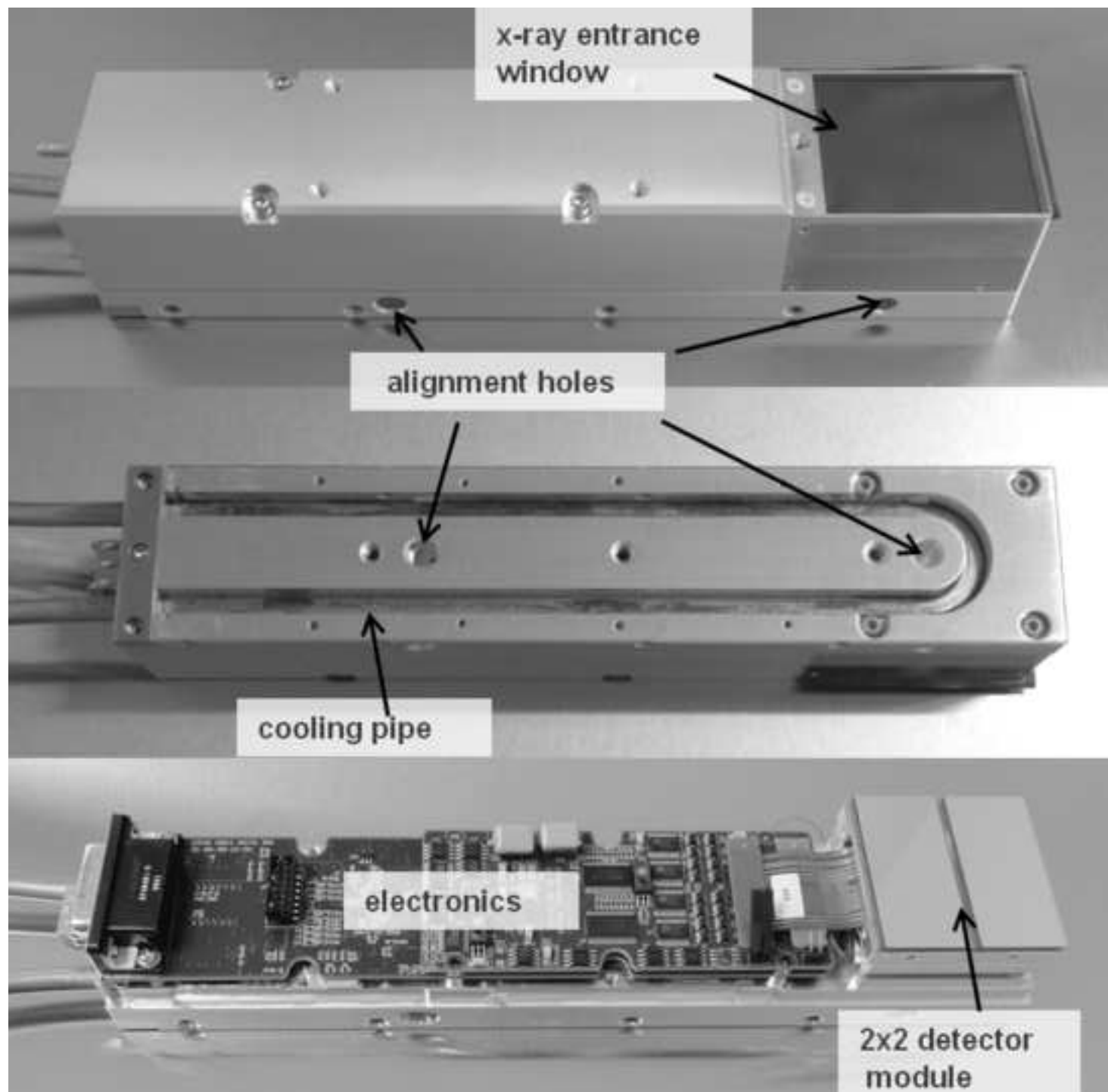


Figure 2  
[Click here to download high resolution image](#)

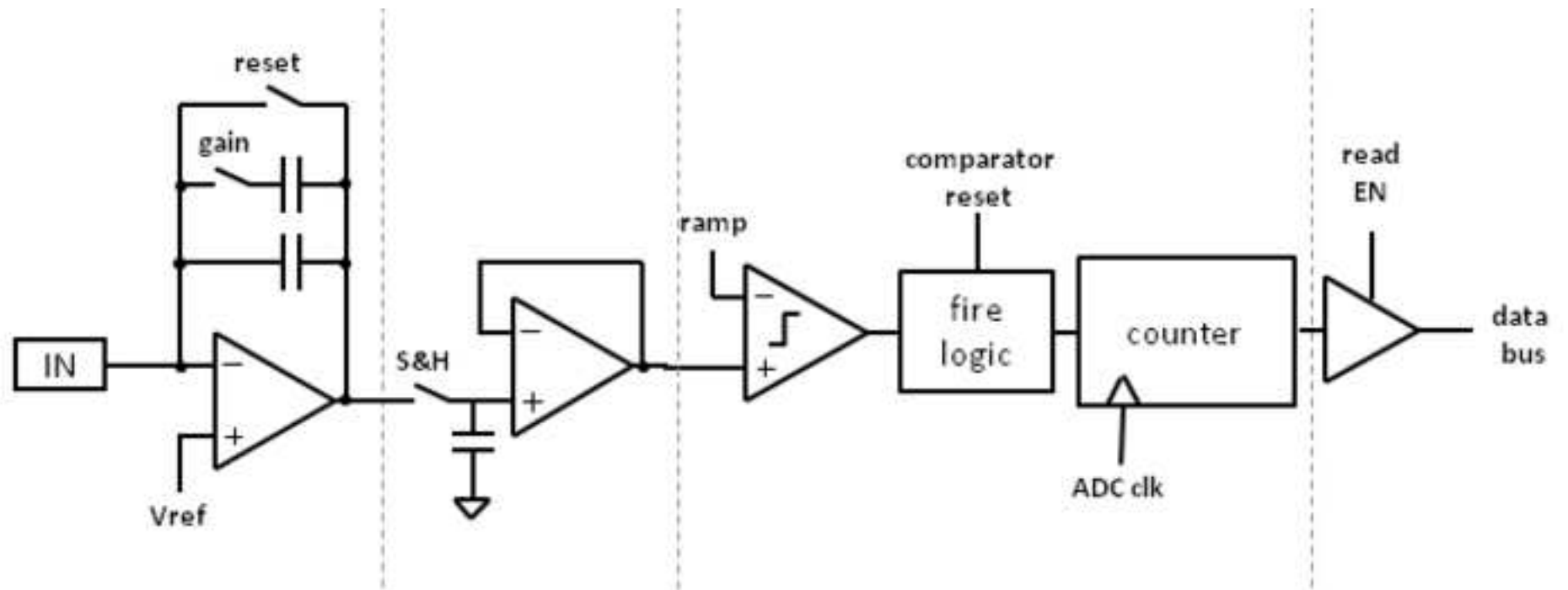


Figure 3  
[Click here to download high resolution image](#)

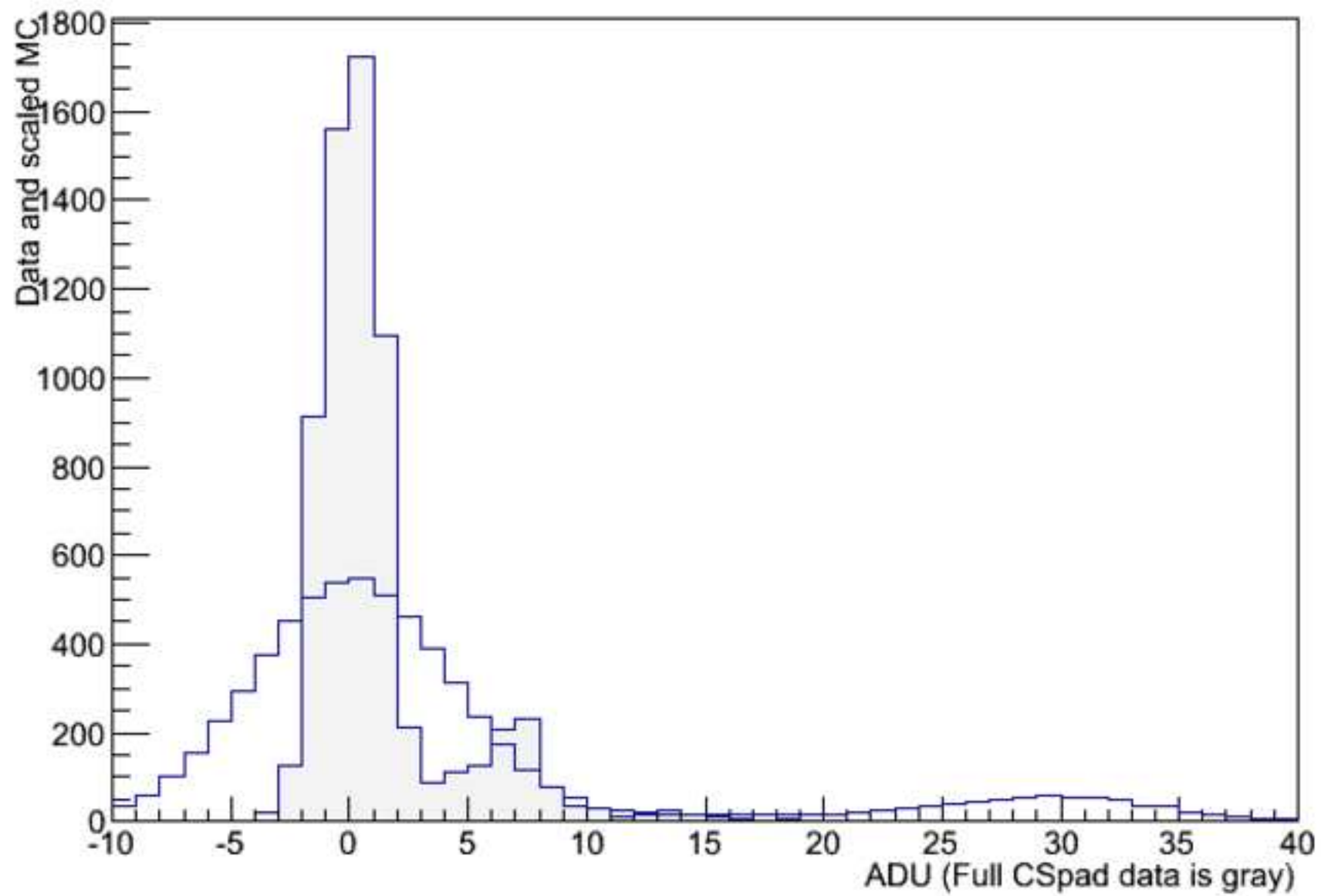




Figure 4  
[Click here to download high resolution image](#)

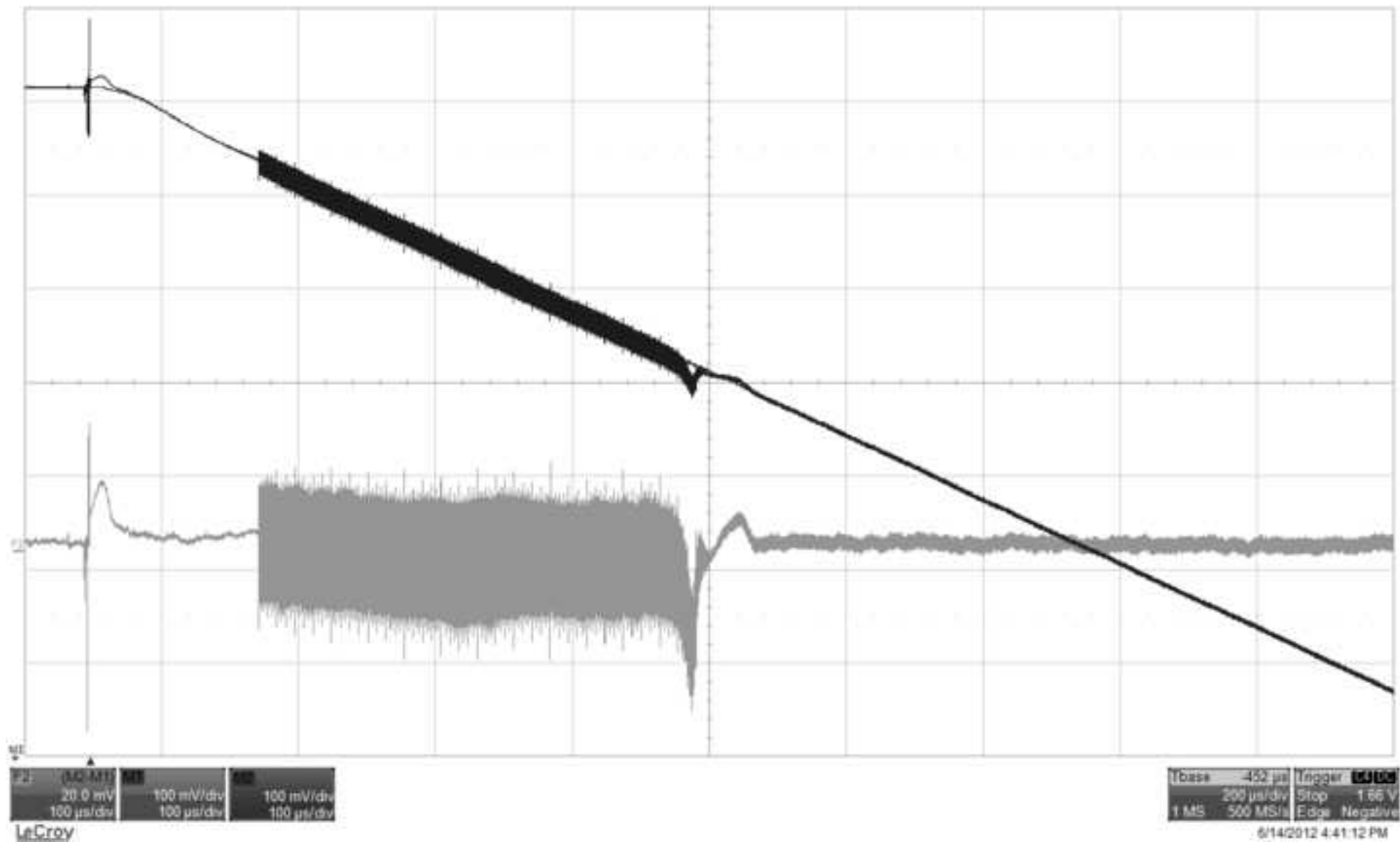


Figure 5  
[Click here to download high resolution image](#)

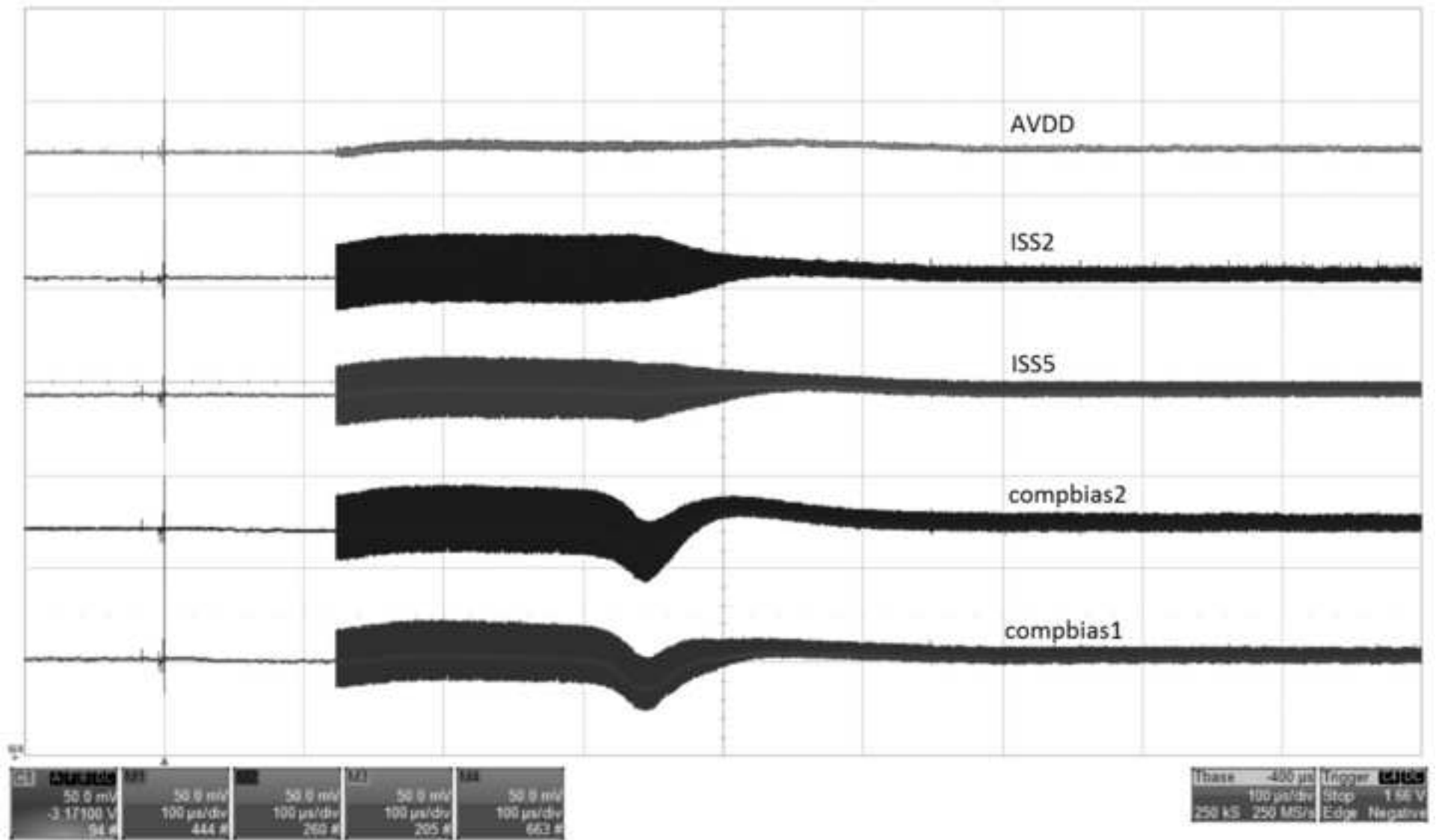


Figure 6  
[Click here to download high resolution image](#)

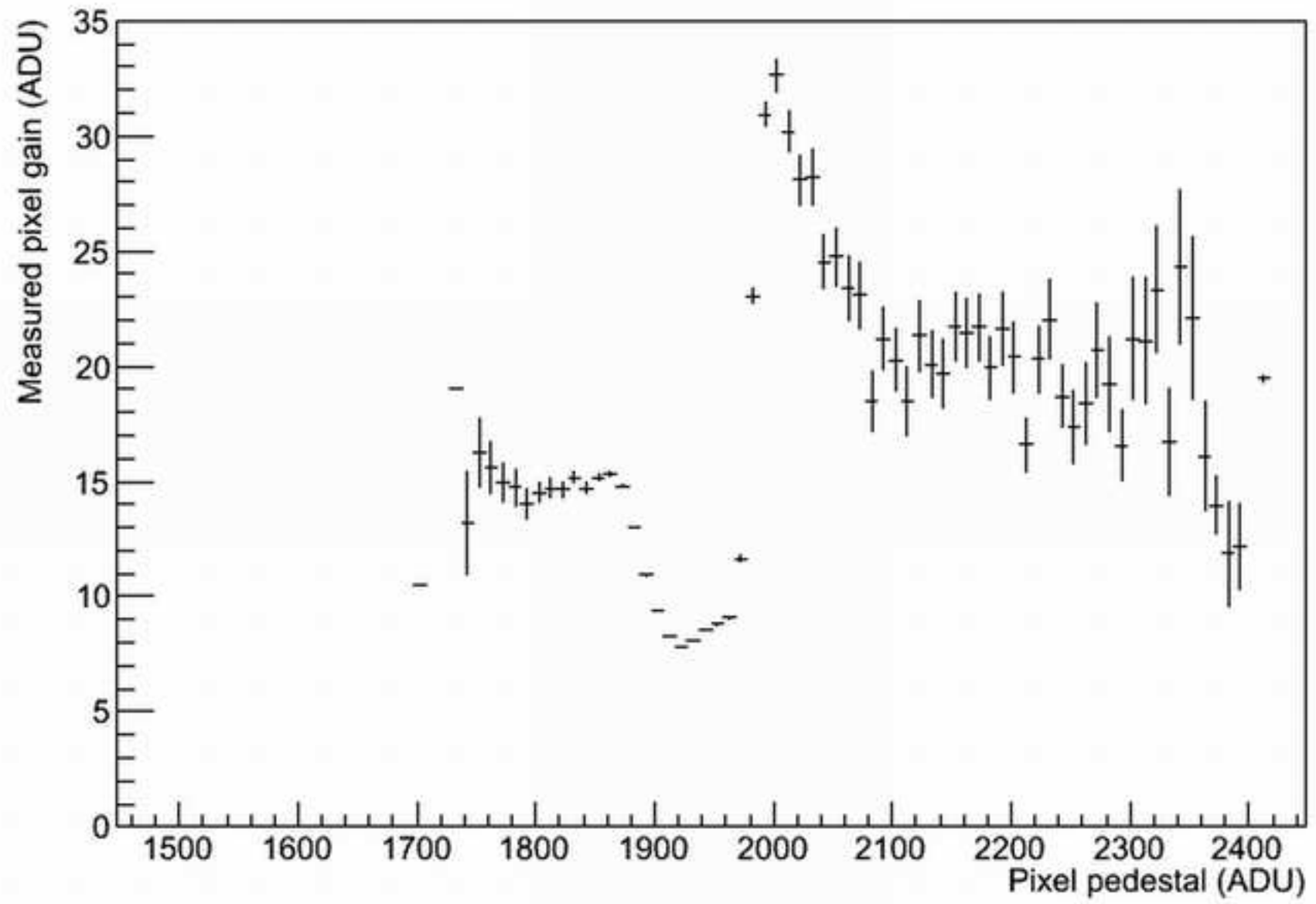


Figure 7  
[Click here to download high resolution image](#)

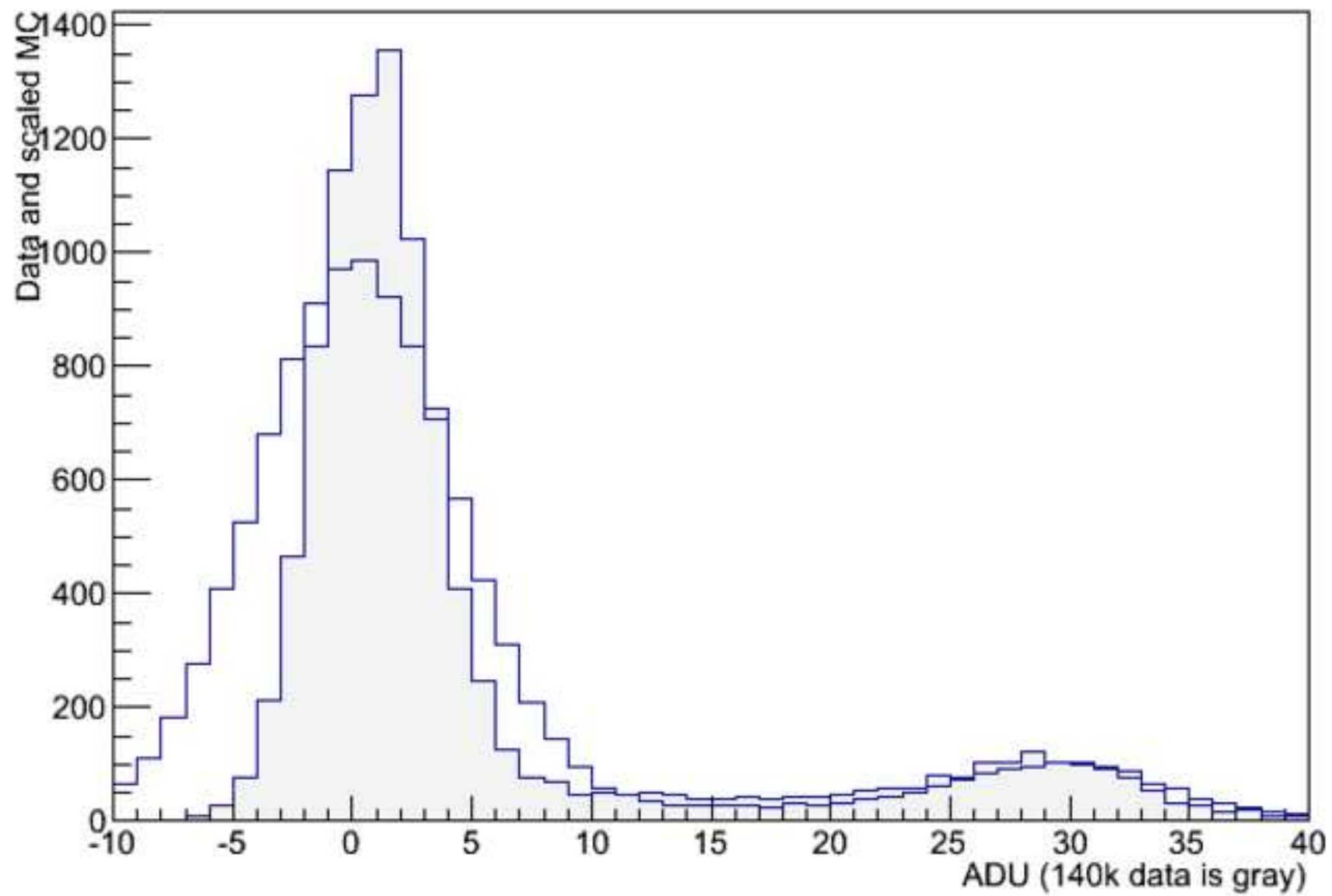


Figure 8  
[Click here to download high resolution image](#)

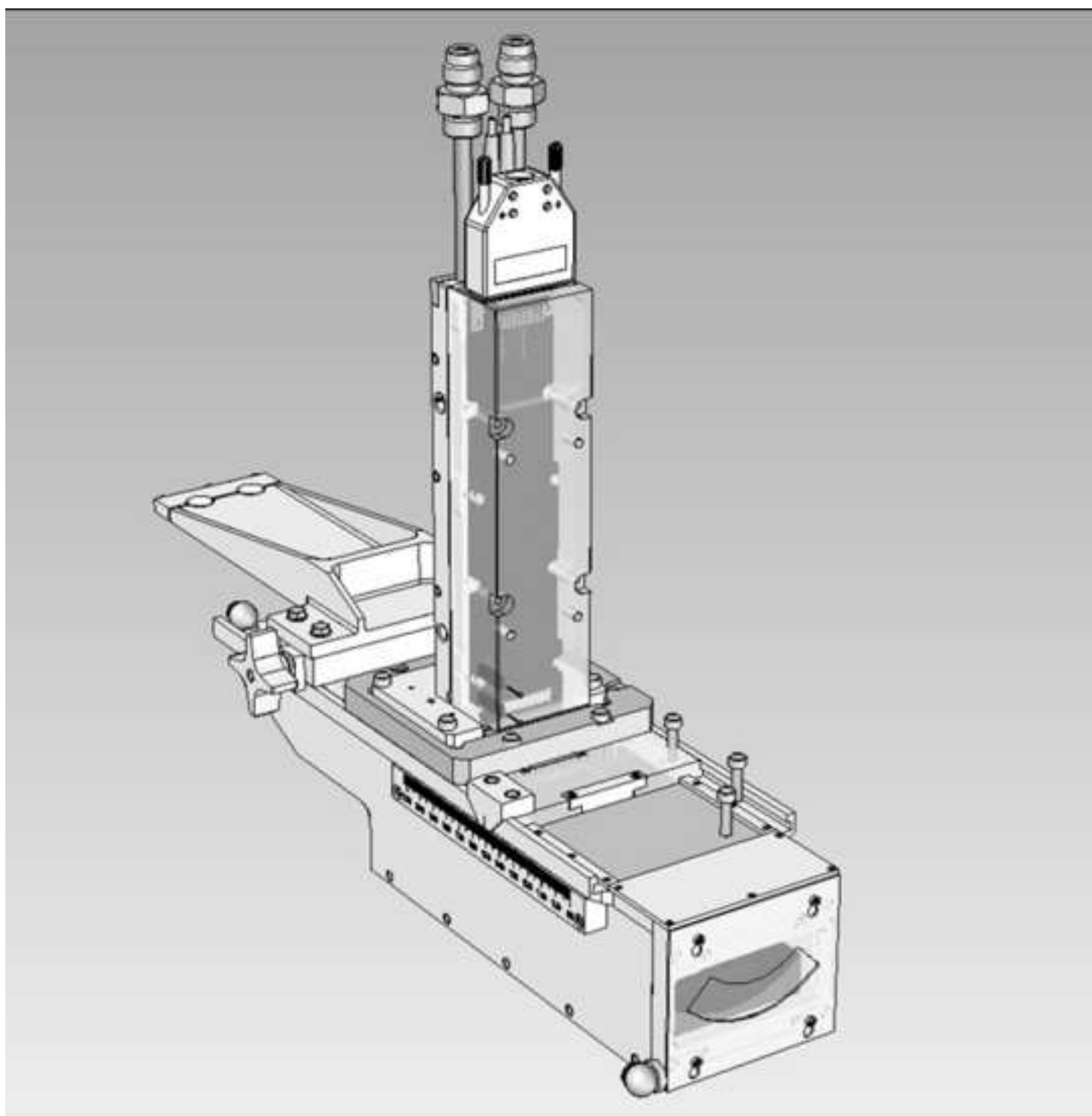


Figure 9  
[Click here to download high resolution image](#)

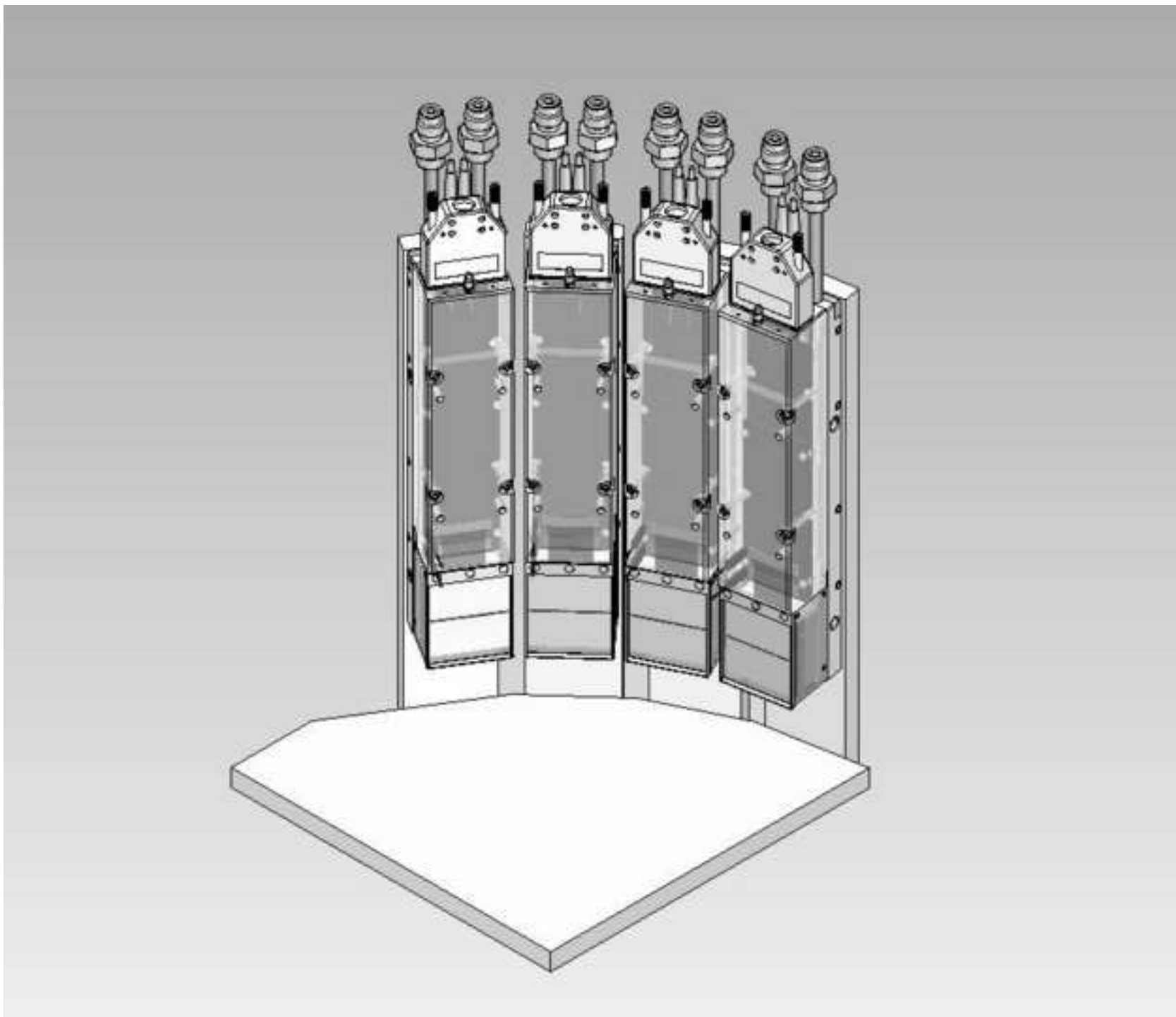


Figure 10 (color)

[Click here to download high resolution image](#)

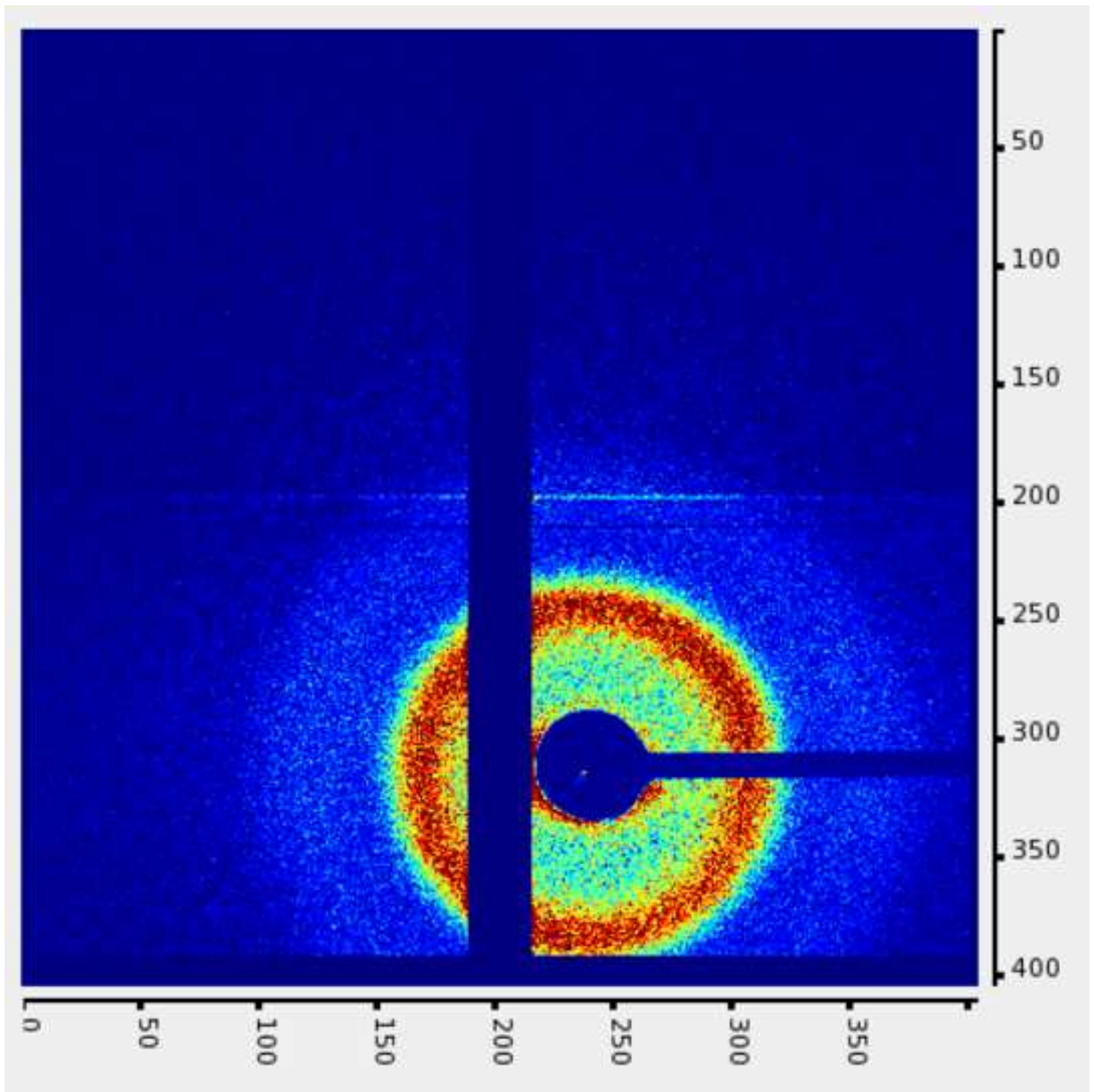


Figure 10 (greyscale)  
[Click here to download high resolution image](#)

